Utilization of waste plum stones as a source of oil and catalyst for biodiesel production

Marija R. Miladinović[1], Stefan Pavlović[2], Ivana B. Banković-Ilić[1], Milan D. Kostić[1], Olivera S. Stamenković[1] and Vlada B. Veljković[1,3]

[1]Faculty of Technology, University of Niš, Bulevar Oslobodjenja 124, 16000 Leskovac, Serbia
[2]University of Belgrade, Institute of Chemistry, Technology, and Metallurgy Center for Catalysis and Chemical Engineering, Njegoševa 12, 11000 Belgrade, Serbia
[3]The Serbian Academy of Sciences and Arts, Knez Mihailova 35, 11000 Belgrade, Serbia

Abstract

Possibilities of using waste plum stones in biodiesel production were investigated. The plum kernels were used as a source to obtain oil by the Soxhlet extraction method, while the whole plum stones, the plum stone shells that remained after the crashing, and the plum kernel cake that remained after the oil extraction, were burned off to obtain ashes. The collected ashes were characterized by elemental composition, porosity, and base strength and tested for catalytic activity in transesterification of esterified plum kernel oil. Dominant elements were potassium, calcium, and magnesium at different contents in the three obtained ashes. The most active catalyst was the plum stone shell ash, so the effect of temperature (40, 50, and 60 °C) on the reaction rate was investigated. The reaction rate constant increased with the reaction temperature with the activation energy value of 58.8 kJ mol^{-1}. In addition, the plum stone shell ash can be reused as a catalyst after recalcination.

Keywords: ash; catalysis; kinetics; methanolysis; transesterification.

Available on-line at the Journal web address: http://www.ache.org.rs/HI/

ORIGINAL SCIENTIFIC PAPER

UDC: 665.75:662.2.03: (634.22+631.53.02)

Hem. Ind. **77(1)** 39-52 (2023)

1. INTRODUCTION

Different waste oily feedstocks, such as used cooking and non-edible oils, have been successfully utilized as suitable raw materials for producing biodiesel [1]. Conversion of these oils into biodiesel is achieved by transesterification with appropriate alcohol (methanol or ethanol) and a suitable homogeneous or heterogeneous acid or base catalyst. Waste biomass ashes occupy a significant place among solid catalytical materials, suitable in terms of environmental parameters, good activity, selectivity, and stability [2]. For example, shells of hazelnuts [3,4] and walnuts [5], produced as waste from the fruit processing industry, were combusted and calcined to ash and then successfully applied as solid base catalysts for sunflower oil methanolysis. In addition, other waste materials, such as salacca and bamboo leave ashes, were used to immobilize ZnO [6] and ZrO_2 [7], respectively, to obtain efficient catalysts for biodiesel production. To consider low-cost solid materials as efficient heterogeneous catalysts, they need to have the following characteristics: high catalytic activity, chemical stability, possibility for easy separation, maintained activity, and reusability [8]. Therefore, the catalytic performance of different biomass ash-based catalysts has recently been tested for biodiesel production under various reaction conditions (Table 1).

Similarly, oils extracted from waste kernels and seeds of different fruits remaining after fruit processing might be alternative, cheap sources for biodiesel production. The oils obtained from kernels or seeds of apricot [9], melon [10], almond [11], pumpkin [12], and mandarin orange [13] were used for biodiesel production by base-catalyzed or two-step acid/base-catalyzed processes.

Plum kernels, as a waste product of food processing, can be a source of inexpensive oil suitable for biodiesel production. The total production of plums in the world in 2020 was over 12 million tons, where China is the largest

Corresponding author: Olivera S. Stamenković, Faculty of Technology, University of Niš, Leskovac, Serbia
E-mail: stamenkovico@tf.ni.ac.rs
Paper received: 13 November 2022; Paper accepted: 25 March 2023; Paper published: 7 April 2023.
https://doi.org/10.2298/HEMIND221113009M

producer, with over 6 million tons per year, while Serbia produces over half a million tons per year [14]. The oil content in plum kernels is 32-46 wt.% [15], and biodiesel quality depends on its fatty acid profile.

Table 1. Biomass ash-based catalysts for biodiesel production

Type of catalyst	Catalyst characteristics	Oil/Alcohol	Reaction conditions				Content/ Yield / Conversion, %	Reuse	Ref.
			MR[a]	C^b / wt.%	t^c / °C	τ^d / h			
Acai seed ash / calcined	Content, % (EDS): K - 12.7, Mg - 2.7, Ca - 1.4, Si - 3.7, P - 3.6, S - 2.0, O - 31.3 Identified crystal phase (XRD): K_2O, SiO_2, CaO, K_2CO_3, K_2SO_4, $CaCO_3$, $Ca_3(PO_4)_2$, MgO, $CaSiO_3$	Soybean oil / Methanol	18:1	12	100	1	98.5 ± 0.21/-/-	1st, 2nd run (92.5%) 3rd, 4th, 5th, 6th run (>80.0%)	[26]
Palm bunch ash / not calcined	Content, % (XRF): K - 81.1, Si - 7.28, Mo - 3.3, Fe - 2.69, Rb - 2.02, P -1.6 Identified crystal phase (XRD): K_2O, CaO, MgO	Palm oil / Methanol	15:1	18	Room	0.5	98.9/-/-	1st run (97.4%) 2nd run (70.2%)	[27]
Banana peel ash / not calcined	Content, % (XRF): K_2O - 65.11, SiO_2 - 0.864, CaO - 7.787, P_2O_5 - 6.068, SO_3 - 2.857, Cl - 2.07 Content, % (EDS): K - 70.06, Ca - 9.54, P -7.55, Si -4.56, Cl -3.23, Mg - 1.78, Fe - 1.49, O - 1.03, S - 0.75 Surface area: 1.4546 $m^2\ g^{-1}$	Soybean oil / Methanol	6:1	0.7	Room	4	-/-/98.95	1st run (98.95%) 2nd run (81.33%) 3rd run (67.74%) 4th run (52.16%)	[28]
Coconut husk ash / not calcined	Identified crystal phase (XRD): K_2O	*Cerbera manghas* oil	6:1	10	60	3	88.6/-/-	1st, 2nd, 3rd, 4th run (88%)	[29]
Pineapple leaves ash / calcined	Identified elements (XRF): K, Ca Identified crystal phase (XRD): MgO, $Mg_2P_2O_7$, $Na_2Ca_4(PO_4)_2SiO_4$, $Al(SO_4)_3$, $Mn_{0.97}Mg_{0.03}SiO_3$, K_2SO_4	Soybean oil / Methanol	40:1	4	60	0.5	-/-/98	1st run (98.92%) 2nd run (97.6%) 3rd run (94.3%) 4th run (> 85%)	[30]
Biomass fly ash / not calcined	Identified elements (EDX): Ca, Mg, Si, Al, O, K, S, Na, Cl, P Content, % (XRD): $CaCO_3$ - 71.0, $Ca(OH)_2$ - 12.9, KCl - 7.1, CaO - 3.8, SiO_2 - 2.3, other - 3.0 Surface area: 9.028 $m^2\ g^{-1}$	Blends of waste cooking oil and refined palm oil /Methanol	6.7 :1	13.57	55	2	-/73.8/-	1st run (73.5%) 2nd run (76.2%) 3rd run (83.6%)	[31]
Walnut shell ash / calcined	Content, wt.% (EDX): K -23.55, Ca -17.67 Identified crystal phase (XRD): CaO, MgO (periclase), SiO_2 (b-cristobalite), K_2O, Ca_2SiO_4, $KAlO_2$, $Ca(OH)_2$ Surface area: 8.8 $m^2\ g^{-1}$ Base strength: $11 < H_- < 15$ Total basicity: 0.352 mmol g^{-1}	Sunflower oil / Methanol	12:1	5	60	0.167	98/-/-	1st, 2nd, 3rd, 4th run (>96%)	[5]

Type of catalyst	Catalyst characteristics	Oil/Alcohol	Reaction conditions				Content/ Yield / Conversion, %	Reuse	Ref.
			MR[a]	*C*[b] / wt.%	*t*[c] / °C	*τ*[d] / h			
Hazelnut shell ash / calcined	Content, wt.% (EDX): K - 26.29, Ca - 11.62, Mg - 6.77, P - 6.10 Identified crystal phase (XRD): $KAlO_2$, $K_4P_2O_7$, K_3FeO_2, Ca_2SiO_4, MgO (periclase), SiO_2 (quartz), CaO and K_2O Surface area: 4.9 $m^2\ g^{-1}$ Base strength: $11 < H\_ < 15$ Total basicity: 1.03 mmol g^{-1}	Used cooking sunflower oil / Methanol	12:1	5	60	0.167	98/-/-	1st, 2nd, 3rd run (>96%)	[3]
Waste fermented-unfermented kola nut pod / calcined	Identified elements (EDX): Ca, K, Mg SFCKNP Base strength: 175 µmol g^{-1} UCKNP Surface area: 0.8 $m^2\ g^{-1}$ Base strength: 140 µmol g^{-1}	Shea butter oil / Methanol	5:1*	2.5	50	0.92	95.30/-/-	1st, 2nd, 3rd run (>95%) 4th run (>90%) 5th run (>85%)	[32]

[a]MR – methanol-to-oil molar ratio; [b]*C* – catalyst loading; [c]*t* – reaction temperature; [d] τ – reaction time; *methanol-to-oil volume ratio; UCKNP - unfermented calcined kola nut pod; SFCKNP - solid fermented calcined kola nut pod

Plum oil has rarely been investigated as a feedstock for biodiesel production. One of the first studies referred to biodiesel synthesis via a two-step process consisting of acid-catalyzed esterification (using H_2SO_4) of free fatty acids followed by base-catalyzed methanolysis (using solid CaO) of the esterified oil, obtained by extraction from plum kernels [16]. Górna *et al.* [17] investigated the potential application of plum kernel oils from twenty-eight varieties of *Prunus domestica* L. and *Prunus cerasifera* Ehrh in the biodiesel industry. The several examined biodiesel properties, such as kinematic viscosity, cetane number, density, and iodine values, satisfied the European biodiesel specification. Almost 70 % of the tested biodiesel samples met the standard for oxidation stability. Composite nano-structured catalysts, obtained by mixing potassium ferricyanide with different low-cost clay support materials such as bentonite, granite, White pocha, Sindh, and Kolten clays, were tested for transesterification of plum kernel oil [15]. Bentonite–potassium ferricyanide composite at a concentration of 0.3 wt.% (reaction conditions: temperature 60 °C, methanol-to-oil molar ratio 10:1) showed a high biodiesel yield, which further increased after calcination of the composite. Also, the obtained biodiesel quality parameters (iodine value, cetane number, acid value, specific gravity, and density) satisfied the standard specifications [15].

Kinetic modeling of homo- or heterogeneously-catalyzed transesterification of different oils has been used for simulation and techno-economic analysis of biodiesel production processes. Kinetic models, such as the second order [18,19], an irreversible pseudo-first-order [20-22], or an irreversible pseudo-second-order [23,24], have been recommended so far. Kostić *et al.* [25] compared kinetic parameters of base-catalyzed methanolysis of different vegetable oils, such as plum kernel, roadside pennycress, olive, melon, grape¬seed, hempseed, and sunflower. Influence of the fatty acid composition of all tested oils on the reaction kinetics was investigated, and the reaction rate constants correlated to the content of unsaturated fatty acids in oils. In addition, the model of the irreversible pseudo-first-order reaction was applied to describe the reaction kinetics. The reaction rate constant increased linearly with increasing the content of unsaturated fatty acids, with the highest value observed for plum oil methanolysis. However, studies about the kinetic modeling of the transesterification reaction of plum oil in the presence of plum stone shell ash as a solid catalyst are lacking.

The present paper is the first attempt to use waste ashes from combustion of the whole plum stone, stone shells, and kernel cake as solid catalysts in methanolysis of plum kernel oil. The possibility of using ash to catalyze methanolysis of oil from the same waste material is advantageous over using other catalysts. Primarily, all catalysts were characterrized by determining their elemental and phase composition and textural parameters. Then, the effect of the reaction temperature on the reaction rate and fatty acid methyl esters (FAMEs) content was investigated. Finally, the kinetics of the methanolysis reaction was analyzed to define the appropriate kinetic model.

2. MATERIAL AND METHODS

2. 1. Materials

Plum fruit was purchased at a local market in South Serbia. The plum stones were used for obtaining the oil and catalyst preparation. The chemicals used in transesterification and analytical analysis were methanol (purity of 99.5 %) obtained from Zorka Pharma (Šabac, Serbia), concentrated sulfuric acid (p.a. 96 %) from Lach-Ner Ltd. (Neratovice, Czech Republic), potassium hydroxide standard solution 0.1 N, Titrisol® from Merck (Darmstadt, Germany), methanol, 2-propanol, and *n*-hexane, HPLC purity, from LGC Promochem (Wesel, Germany), phenolphthalein, thymolphthalein, thymol violet, 2,4-dinitroaniline and benzene carboxylic acid (Sigma Aldrich, USA).

2. 2. Oil extraction

Plum kernel oil was obtained by the Soxhlet extraction method [16]. The yield of obtained oil was 332±02 g / kg with a moisture content of 2.7±0.1 wt.% and an acid value of 14.7±0.1 mg KOH/g. Due to its high acid value, the oil was pre-esterified. The presence of free fatty acids (FFA) is not desirable in base-catalyzed transesterification due to the possibility for catalyst consumption. Usually, refined oils with an acid value lower than 2 mg KOH/g are recommended [33]. The esterification of plum kernel oil was carried out at optimal reaction conditions defined by Kostić *et al.* [16] to reduce its acid value to 1.0±0.2 mg KOH/g making it suitable for base-catalyzed transesterification.

2. 3. Catalyst preparation

Three types of catalysts were prepared by burning off the whole plum stones, stone shells, and kernel cake in open air. The obtained chars were calcined in a furnace at 800 °C in the air atmosphere, resulting in 3 wt.% of ash content. Catalytic activity of the calcined ashes obtained from plum stones (PSA), stone shells (PSSA), and kernel cake (PKCA) was tested in transesterification of plum oil with methanol.

2. 4. Catalyst characterization

2. 4. 1. Elemental analysis

Elemental analysis of ashes was determined by using the inductively coupled plasma analytical technique with optical emission spectrometry (ICP-OES). Digestion of samples was carried out in a microwave digester (Ethos 1, Milestone, Italy), in closed Teflon cuvettes, at high pressure (10 MPa) and high temperature (210 ^{o}C) for 20 min. Acids used for the total sample dissolution were H_2SO_4 96 %, H_3PO_4 85 %, HNO_3 65 %, and HF 40 % (Alfa Aesar GmbH & Co KG, Germany). For instrument calibration, standard solutions were prepared from the multi-element standard plasma solution 4, Specpure®, 1000 µg cm^{-3}, and silicon, the standard plasma solution, Specpure®, Si 1000 µg cm^{-3} (Alfa Aesar GmbH & Co KG, Germany). The concentration of elements was measured by using an iCAP 6500 Duo ICP instrument (Thermo Fisher Scientific, Cambridge, UK) with iTEVA operating software.

2. 4. 2. XRD analysis

Identification of phases in PSA, PSSA, and PKCA samples was performed by the X-ray powder diffraction (XRD) technique (Rigaku SmartLab automatic multipurpose X-ray diffractometer) using CuKα radiation (λ = 0.15418 nm) in the 2θ range of 10-90° and step-length of 3^{o} min^{-1}. The crystalline phases were identified by comparing the XRD diffractograms with the diffraction patterns of individual phases provided by the ICDD (International Center for Diffraction Data), the former JCPDS (Joint Committee of Powder Diffraction Standards).

2. 4. 3. Hg porosimetry

Mercury Intrusion Porosimetry measurements were performed in the fully automated conventional apparatus Carlo Erba Porosimeter 2000 (Carlo Erba, Italy; pressure range: 0.1 to 200 MPa; pores with a diameter within 7.5 and 15,000 nm). Acquisition of the analysis data was performed by using the Milestone Software 200 (Milestone Systems, Denmark). Two subsequent intrusion-extrusion runs (Run I and Run II) were conducted. Before the analysis, the samples were evacuated for 2 h in a dilatometer placed in the Macropores Unit 120 (Carlo Erba, Italy).

2. 4. 4. Base strength

Base strength (*H_*) of catalysts was determined by using Hammett indicators: phenolphthalein (*H_* = 9.3), thymolphthalein (*H_* = 10.0), thymol violet (*H_* = 11.0), and 2,4-dinitroaniline (*H_* = 15.0). The procedure included mixing the catalyst (50 mg) with 1 cm^3 of Hammett indicators solution diluted in 2 cm^3 of methanol. The mixture was shaken for 1 h and left to reach color equilibration. The base strength of the catalyst was determined based on the change of color in the solution. The change of colors occurs when the catalyst strength is higher than the weakest indicator, but it remains unchanged when it is lower than the strongest indicator. The catalyst basicity was measured by titration of the Hammett indicator-benzene carboxylic acid (0.02 mol L^{-1} anhydrous ethanol solution).

2. 5. Transesterification

Transesterification of esterified plum kernel oil (20 g) with methanol (8.83 g) using PSA, PSSA, PKCA as a catalyst (catalyst loading of 10 %, based on the oil weight) was carried out in a 250 cm^3 three-neck glass round-bottom flask equipped with a reflux condenser and stirred by a magnetic stirrer. The initial methanol-to-oil molar ratio of 12:1 was kept constant while the reaction temperature varied from 40 to 60 °C. The reaction mixture was intensively agitated at 800 rpm. The samples (0.3 cm^3) were taken at timed intervals (5, 10, 20, 30, 40, 50, 60, 75, 90, and 120 min) and quenched by immersing the vials in ice water and centrifuged (Sigma Laborcentrifugen 2-6E, Germany, 3500 rpm) for 10 min to separate the methyl ester layer. The upper layer aliquot (methyl esters phase) was dissolved in a solution of 2-propanol and *n*-hexane (5/4, v/v) in the ratio of 1:200 and filtered through a 0.45 μm Millipore filter to prepare for HPLC analysis. The HPLC analysis was performed by using HPLC chromatography (Agilent 1100 Series, Agilent Technologies, Germany) according to the method described elsewhere [34]. The test for catalyst reusability was also performed under the same reaction conditions: the catalyst amount of 10 wt.%, the methanol-to-oil molar ratio of 12:1, and the reaction temperature of 60 °C. The catalyst was separated from the reaction mixture at the end of reaction by vacuum filtration and used in the next batch without treatment. Also, the separated catalyst was recalcined (800 °C, 2 h) before the subsequent cycle and then tested for reusability. All experiments were done in duplicate.

3. KINETICS

Kinetics of plum oil methanolysis catalyzed by PSSA was studied under intensive agitation (800 rpm) at various temperatures by monitoring the FAME production. It was assumed that the catalyst, reactants, and products were distributed uniformly in the reaction mixture. As a result, the consumption rates of diacylglycerols (DAGs) and monoacylglycerols (MAGs) were higher than that of triacylglycerols (TAGs), resulting in low concentrations of the two former acylglycerols during the reaction. Hence, the conversion of plum kernel oil into the FAMEs and glycerol, in the presence of ash as a solid catalyst, can be presented by the overall stoichiometric equation instead of presenting separately each of all three reaction steps, equation (1):

$$A + 3B \rightleftarrows 3R + S \quad (1)$$

where A, B, R, and S denote the reactants and products: oil, methanol, FAME, and glycerol, respectively.

The reaction occurred in excess of methanol, so it can be considered irreversible. At lower temperatures, the overall process rate is controlled by the TAG mass transfer rate and the chemical reaction rate in the initial heterogeneous and the later pseudo-homogeneous regime, respectively [35]. On the other hand, only a pseudo-homogeneous regime exists at the highest temperature, where the chemical reaction limits the overall process rate. The pseudo-first-order kinetic model is valid for both heterogeneous and pseudo-homogeneous regimes [35], equation (2):

$$\left(-r_A\right) = -\frac{\mathrm{d}c_A}{\mathrm{d}\tau} = kc_A \quad (2)$$

where c_A is the TAG concentration, k is the apparent rate constant, and τ is the reaction time. For the heterogeneous regime, the apparent rate constant corresponds to the TAG mass transfer coefficient. For the pseudo-homogeneous regime, it is the pseudo-first-order reaction rate constant. The TAG concentration is related to the conversion degree x_A as follows, equation (3):

$c_A = c_{A0}(1-x_A)$ (3)

By introducing Eq. (3) into Eq. (2) and by integrating it for the initial condition: $\tau = 0$ and $x_A = 0$, the final equation (4) is obtained:

$-\ln(1-x_A) = k\tau + C$ (4)

where C is the integration constant ($C = 0$ for the heterogeneous regime at 40 and 50 °C and the pseudo-homogeneous regime at 60 °C, because $x_A = 0$ for $\tau = 0$).

4. RESULTS AND DISCUSSION

4. 1. Catalyst characterization

The main elements in the obtained ashes were K, Ca, and Mg (Table 2), at reasonably high contents typical for some ashes, such as *Sesamum indicum* plant ash [36], hazelnut shell ash [3] or *Acai* seed ash [26]. Silicon, a common constituent of ashes from various sources, such as wood, shells, straws, and husks [37], was present in the PSA and PSSA but significantly less in PKCA. The prevalence of K and Ca affects the catalytic activity of ash. A high FAME content was achieved in a shorter reaction time in oil methanolysis catalyzed by ashes containing higher contents of K and Ca than other elements [3,5,26]. Similarly, a higher ash catalytic activity due to the presence of K was demonstrated by comparing the catalytic activities of hazelnut shell ash and quicklime (CaO) under similar reaction conditions [3].

Table 2. Elemental composition of the obtained ashes

Element	Content*, %		
	PSA	PSSA	PKCA
Ca	9.43	11.79	6.55
K	7.82	11.31	12.47
Mg	2.62	2.43	3.08
Si	1.07	2.49	0.05
Fe	0.71	0.68	0.08
Al	0.48	0.58	0
Na	0.32	0.47	0.14

*STD was lower than 0.26

The structure evolution during calcination of raw materials is shown in Fig. 1. The detected crystalline phases in all three samples could be divided into three groups: group I – pure oxide and chloride phases of potassium (sylvite – KCl, PDF#41-1476), calcium (lime – CaO, PDF#37-1497), magnesium (periclase – MgO, PDF#43-1022), and silicon (quartz – SiO_2, PDF#46-1045), group II – calcium silicate phases (rankinite – $Ca_3Si_2O_7$, PDF#22-0539 and laranite – Ca_2SiO_4, PDF#70-0388), group III – complex crystalline phases of potassium, magnesium, calcium, sodium, aluminum, and silicon in the form of sulfate, phosphate, and chloride (hazenite – $KNaMg_2(PO_4)_2 \cdot 14H_2O$, PDF#15-0762, kainite – $KMg(SO_4)Cl \cdot 2.75H_2O$, PDF#35-0812, carnallite - $KMgCl_3 \cdot 6H_2O$, PDF# 24-0869, polyhalite – $K_2Ca_2Mg(SO_4)_4 \cdot 2H_2O$, PDF#5-628, syngenite –$K_2Ca(SO_4)_2 \cdot \cdot H_2O$, PDF#74-2159 and flörkeite – $K_3Ca_2Na[Al_8Si_8O_{32}] \cdot 12H_2O$, PDF#34-0137). The phase composition corresponds to the other ashes derived from different biomass sources [38]. Intensities of the primary diffraction line of phases varied according to chemical composition and decreased as the element concentration decreased. However, interactions between elements led to a deviation due to the creation of numerous complex phases. The appearance of group II characteristic phases follows the mechanism of biomass ash formation [38] as a consequence of the interaction between CaO and SiO_2 during the solid-state reaction at the ash fusion temperature. At high temperatures (>700 °C), CaO penetrates the melted glassy phase, whereby a part reacts and forms calcium silicate compounds. The other part of CaO is trapped and inaccessible as an active catalyst center. More significant calcium losses at these temperatures are characteristic for samples with higher silicon contents and for long-term calcination [39]. Besides the simple compounds in the CaO-SiO_2 phase system, creation of more complex crystal forms (group III) takes place, especially in the case of a sample with the low silicon content. The crystalline phases from groups II and III could contribute to the morphological and textural properties of the final catalyst.

The values of textural parameters obtained by Hg porosimetry for the obtained catalysts (*i.e.* calcined ashes) are given in Table 3. Furthermore, the total intruded volume of Hg and the corresponding pore size distribution (PSD) curves for the two subsequent intrusion cycles (I and II) are presented in Fig. 2. In all three samples, a significant reduction in the total intruded mercury can be observed, indicating the existence of interparticle space in the materials [40], which was confirmed by a decrease in porosity amounting to 40 to 65 % in the cycle II. The PSD curve for the PSA sample is bimodal in cycle I with pore diameters centered at 2.48 and 7.53 μm. In cycle II, the PSD curve exhibits a monomodal character with a pore diameter centered at 2.23 μm.

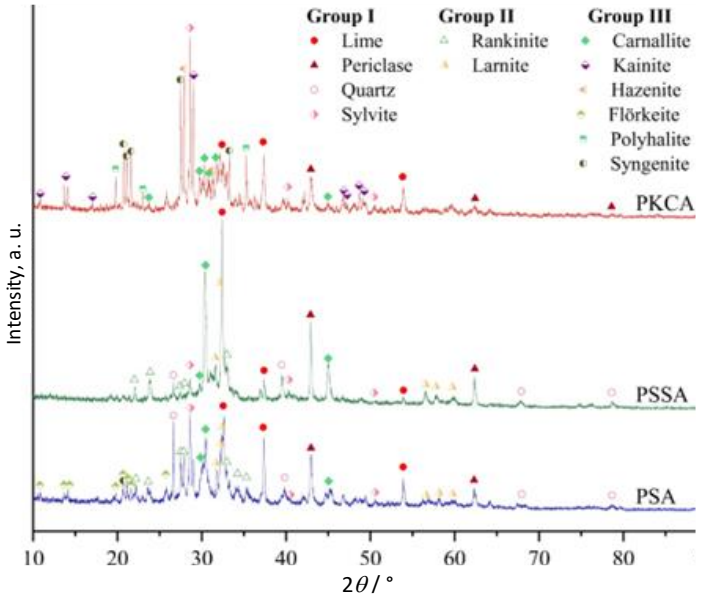

Fig. 1. XRD patterns of calcined PSA, PSSA and PKCA ashes

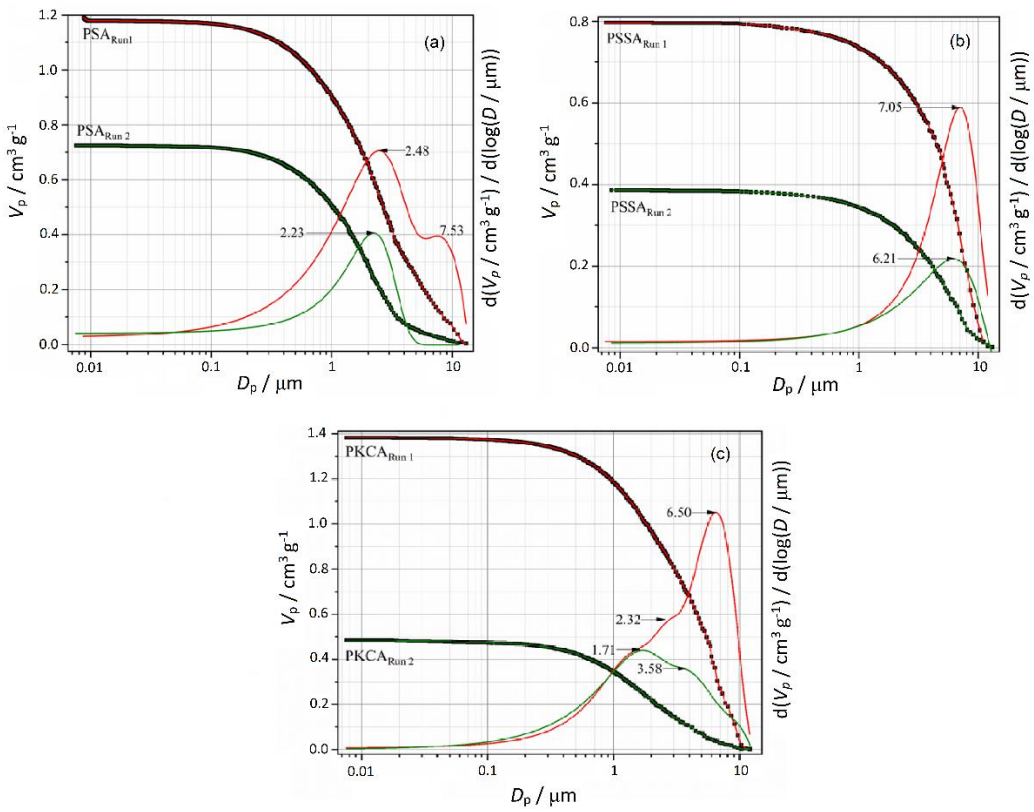

Fig. 2. Pore size distribution curves for (a) PSA, (b) PSSA, and (c) PKCA ashes

On the other hand, the PSD curves for the PSSA sample exhibit monomodal character in both intrusion cycles with a slight change in pore diameter centered at nearly 7.0 μm. Unlike the first two samples, the PSD curves for PKCA are multimodal with pore diameters in a wide range (from 1.71 to 6.50 μm). The multimodal character of the curve was preserved in the cycle II but with a somewhat narrower range of pore diameters, excluding pores of about 7.0 μm. Shifting pore size to a larger diameter leads to a lower surface area [41]. Thus, the pore diameter for all samples is in the macropore region, as confirmed by a low specific surface area. The macroporous pore system is very favorable and suitable for reactions whose reactants are large organic molecules, such as TAGs [3,5,42]. However, for the type of catalyst obtained in the one-way process, such as in this study, the chemical composition plays a more significant role than the textural properties. Although the catalytic activity of solid catalysts is directly related to the surface area, the surface area did not influence the catalytic activity of walnut and hazelnut ashes [3,5]. The PSSA catalyst had the lowest surface area (Table 3) amounting to 1.67 $m^2 g^{-1}$, which is lower than the value reported for a *Sesamum indicum* plant ash (3.66 $m^2 g^{-1}$) [36] and close to that of a *Musa acuminata* peel ash (1.45 $m^2 g^{-1}$) [28].

The base strength ($H\_$) for all catalysts was in the range $9.3<H\_<15.0$. The PSSA sample exhibited the highest basicity (3.384 mmol g^{-1}), while the basicity of the PKCA and PSA samples was lower (1.293 and 0.924 mmol g^{-1}, respectively).

Table 3. Textural parameters of catalysts

Sample	Intrusion cycle	V_p / $cm^3 g^{-1}$	S_{Hg} / $m^2 g^{-1}$	D_p / μm	BD / g cm^{-3}	BD_{Corr} / g cm^{-3}	P / %
PSA	I	1.19	10.35	2.60	0.67	3.31	79.75
	II	0.73	3.83	2.27	0.67	1.30	48.58
PSSA	I	0.80	1.67	7.23	0.93	3.59	74.06
	II	0.39	1.28	5.05	0.93	1.45	35.93
PKCA	I	1.38	4.14	5.81	0.57	2.69	78.83
	II	0.49	3.16	1.67	0.57	0.79	27.65

V_p – Total pore volume; S_{Hg} – Specific surface area; D_p – Average pore diameter; BD – Bulk density; P - Porosity

4. 2. Plum kernel oil methanolysis catalyzed by PSA, PSSA, and PKCA ashes

The catalytic performance of PSA, PSSA, and PKCA was evaluated in methanolysis of the pre-esterified plum oil. Change in FAME contents during the reactions is presented in Fig. 3, where the order of the catalytic performance of the tested ashes was PSSA > PKCA > PSA and it follows their basicity. Significantly higher FAME contents were achieved in the reaction catalyzed by PSSA as compared to those obtained in the reactions catalyzed by PSA and PKCA during the whole reaction period. Furthermore, rapid formation of FAMEs in the initial reaction period contributed to a faster overall reaction catalyzed by PSSA, thus indicating absence of diffusion limitations in the liquid-liquid-solid system at the beginning of the reaction. On the other hand, slow FAME formation at the beginning of the reactions catalyzed by PSA or PKCA was evident.

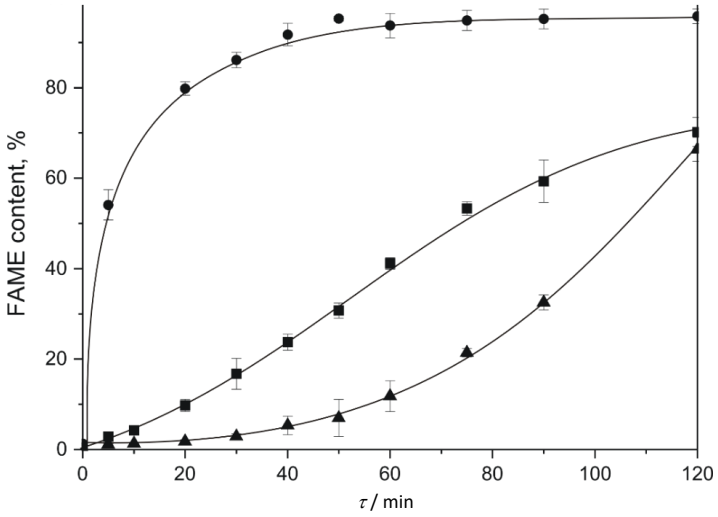

Fig. 3. Methanolysis of plum kernel oil catalyzed by PSSA - ●, PSA - ▲ and PKCA - ■ (reaction temperature 60 °C)

Investigating the catalytic performance of mixed oxides, Fraile *et al.* [43] found that alkaline ions (Na^+) were the primary source of the catalyst strong basicity and contributed to the higher catalytic activity. Furthermore, they concluded that solids with a high content of alkaline ions had a low surface area. Therefore, the observed difference in reaction rates could be analyzed from the aspect of elemental composition; the higher content of Ca and K would positively affect the basicity. Buchori *et al.* [44] studied the effect of adding K_2O to CaO-ZnO on the resulting catalyst basicity. The results revealed that a higher molar ratio of CaO and higher content of the added K_2O increased the catalyst basicity. Similarly, Tang *et al.* [45] reported that loading KCl onto CaO can increase the basicity of the catalyst and affect its porosity. Although the pore size diameters of all catalysts investigated in the present study were distributed in the macroporous region (Section 4. 1.) indicating effective diffusion [41], lower reaction rates of the reactions catalyzed by PKCA and PSA were observed.

4. 3. Effect of the reaction temperature on the methanolysis reaction rate and FAME content

Since PSSA showed the best catalytic performance, kinetics of the reaction catalyzed by this catalyst was investigated at three reaction temperatures (40, 50 and 60 °C). Lower FAME contents were achieved when the reaction was performed at lower temperatures (Fig. 4), which was especially pronounced in the initial reaction period. A longer reaction time was required to reach the FAME content over 95 % at 50 °C than at 60 °C. Similarly, Barros *et al.* [30] found that increasing the temperature from 50 to 60 °C significantly increased the FAME content in the reaction catalyzed by calcined pineapple leaves ash. The increase in the reaction temperature increases the reaction rate constant since oil methanolysis is an endothermic reaction. However, by lowering the reaction temperature, diffusion limitations in the liquid-liquid-solid system could also occur, causing a slow initial reaction period. A temperature increases from 40 to 80 °C at a methanol-to-oil molar ratio of 12:1 and a catalyst loading of 7 wt.% positively affected oil conversion over calcined tucumã peel ash, containing mainly K, P, Ca, and Mg [46]. The PSSA-catalyzed methanolysis was performed at a lower temperature (60 °C) than other methanolysis reactions catalyzed by different ashes reported in literature [35,46-48]. Likewise, the high FAME contents were achieved at the same reaction temperature in oil methanolysis using the walnut shell [5] and hazelnut shell [3] ashes as catalysts.

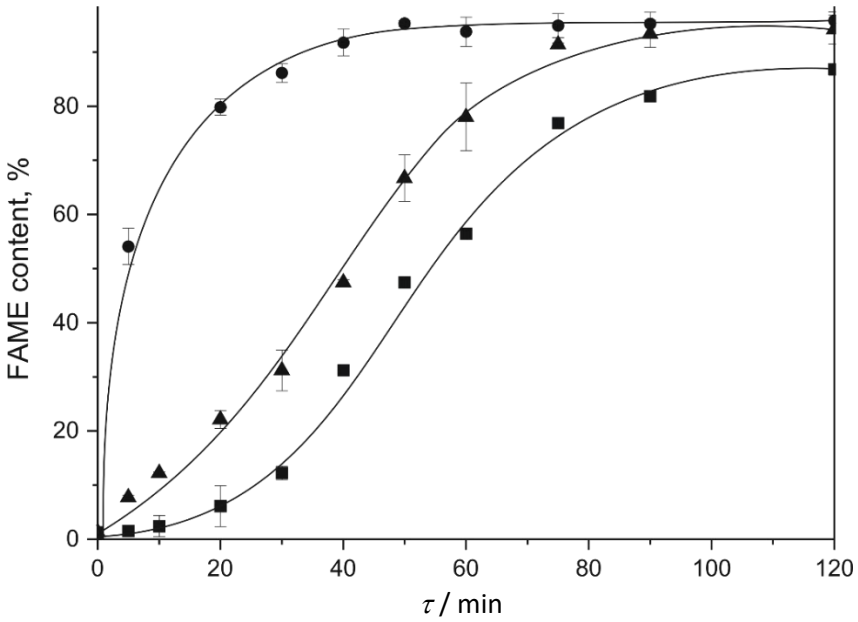

Fig. 4. Changes in the FAME content over the reaction time at different reaction temperatures: 60 °C - ●, 50 °C - ▲ and 40 °C - ■

A simple empirical pseudo-first-order reaction model (Eq. 4) was employed for the kinetic study of plum oil methanolysis catalyzed by PSSA. The dependence -ln (1-x_A) *vs*. time is shown in Fig. 5. The reaction performed at 60 °C was successfully described by the model as a linear dependence -ln (1-x_A) *vs*. time was observed. However, for the reactions at 40 and 50 °C, two straight lines with different slopes in the initial and the final reaction periods were observed. Therefore,

Eq. (4) was applied to calculate only the apparent reaction rate constants for the pseudo-homogeneous regime at different temperatures. The apparent reaction rate constant increased with the temperature (Fig. 6). The activation energy for the plum oil methanolysis catalyzed by PSSA was calculated by applying the Arrhenius equation (5):

$$k = Ae^{\left(-\frac{E_a}{RT}\right)} \quad (5)$$

where A / min^{-1}is the pre-exponential factor, E_a / J·mol^{-1} is the activation energy, R is the gas constant (8.314 J·mol^{-1}·K^{-1}), and T / K is the reaction temperature.

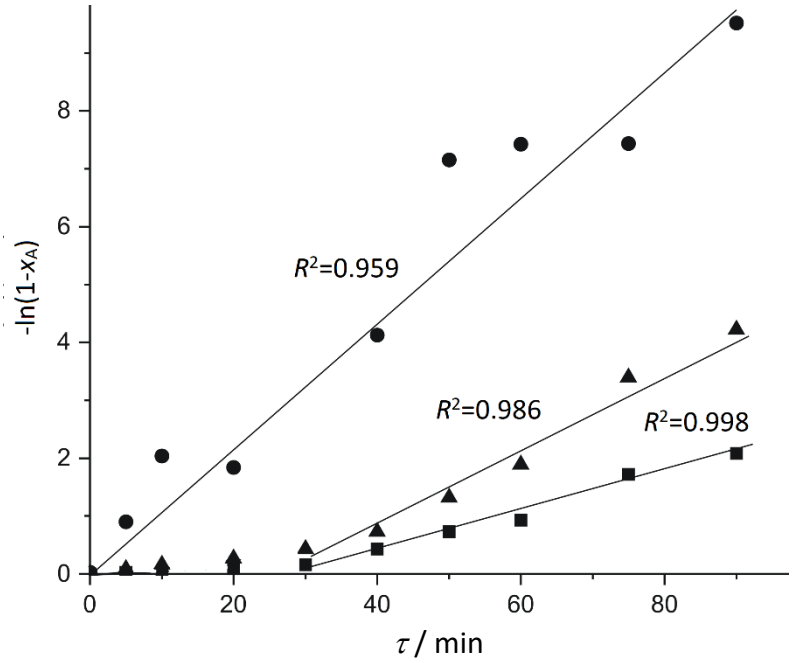

Fig. 5. Application of the irreversible pseudo-first-order kinetic model (lines) for plum kernel oil methanolysis at different reaction temperatures (experimental data: 60 °C - ●, 50 °C - ▲, and 40 °C - ■)

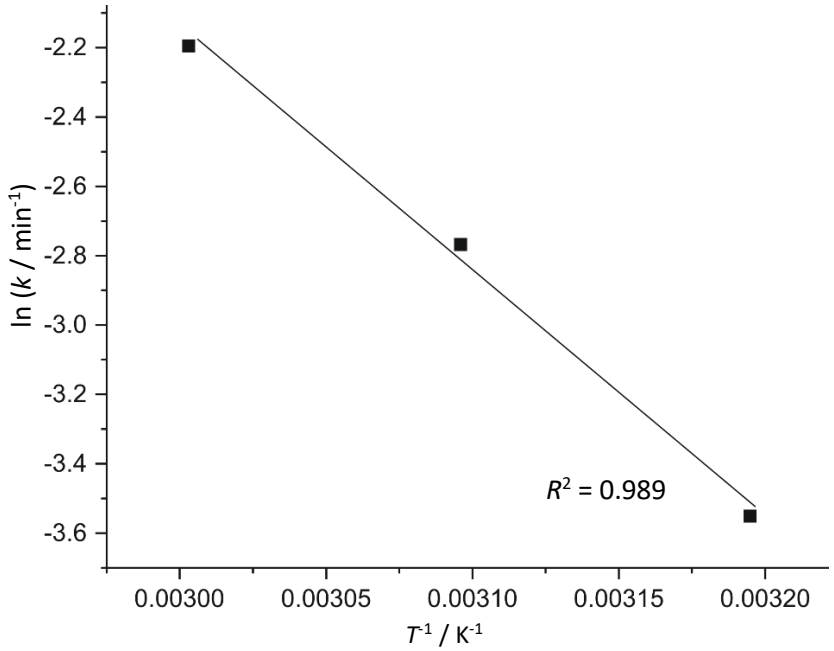

Fig. 6. Dependence of ln k on the 1/T (Arrhenius plot)

The values of ln *k* were linearly dependent on 1/*T*, as shown in Fig. 6 and the activation energy was calculated from the slope of the linear dependence. Hence, the activation energy and pre-exponential factor of plum oil methanolysis catalyzed by PSSA were determined to be 58.8 kJ mol^{-1} and $19.3 \cdot 10^5$ min^{-1}. The activation energy value was in the range of other values reported in literature, presented in Table 4. It is lower than the values for methanolysis of soybean oil catalyzed by pineapple leaves ash [30] and *Tucumã* peel ash [46] but higher than those reported for methanolysis of *J. curcas* oil and soybean oil catalyzed by *L. perpusilla* Torrey ash [49] and waste *Brassica nigra* plant ash [52], respectively.

Table 4. Summary of activation energy values reported for oil methanolysis catalyzed by various solid base catalysts

Catalyst type	Type of oil feedstock	Kinetic model	E_a / kJ mol^{-1}	Ref.
L. perpusilla Torrey ash	*Jatropha curcas* L. oil	Based on TGA analysis	29.49	[49]
Palm oil mill fly ash supported calcium oxide	Crude palm oil	Pseudo-first order	42.56	[50]
Rice husk-derived sodium silicate	Palm oil	Pseudo-first order	48.30	[51]
Tucumã peel ash	Soybean oil	Pseudo-first order	61.23	[46]
Waste *Brassica nigra* plant ash	Soybean oil	Pseudo-first order	27.87	[52]
Pineapple leaves ash	Soybean oil	n.r.	86.84	[30]
Citrus sinensis peel ash (CSPA)@Fe_3O_4	Waste cooking oil	Pseudo-first order	34.41	[53]
Plum stone shell ash	Plum oil	Pseudo-first order	58.8	This work

n.r. – not reported

4. 4. Reuse of the PSSA catalyst

The PSSA catalyst was tested for reuse as it exhibited the highest catalytic activity. After the reaction completion the catalyst was separated from the reaction mixture and reused in the next batch without treatment. In the repeated reaction a low FAME content (30 %) was obtained at 60 min, indicating the catalytic activity loss. Therefore, the separated catalyst was recalcined (800 °C, 2 h) before the subsequent cycle. In this case, a high FAME content of 93.54 % was achieved in 90 min of reaction (Fig. 7), which was still lower than that achieved in the first batch. Similarly, a lower FAME content at the beginning of the reaction was observed with recalcined walnut and hazelnut shell ashes [3,5]. Therefore, PSSA could be recommended as an effective catalyst for the transesterification of plum kernel oil with the possibility of being reused after recalcination. However, a further detailed investigation of reused catalysts in respect of basicity and elemental and phase composition should be performed to provide information on the effect of the reuse and recalcination on the catalytic activity.

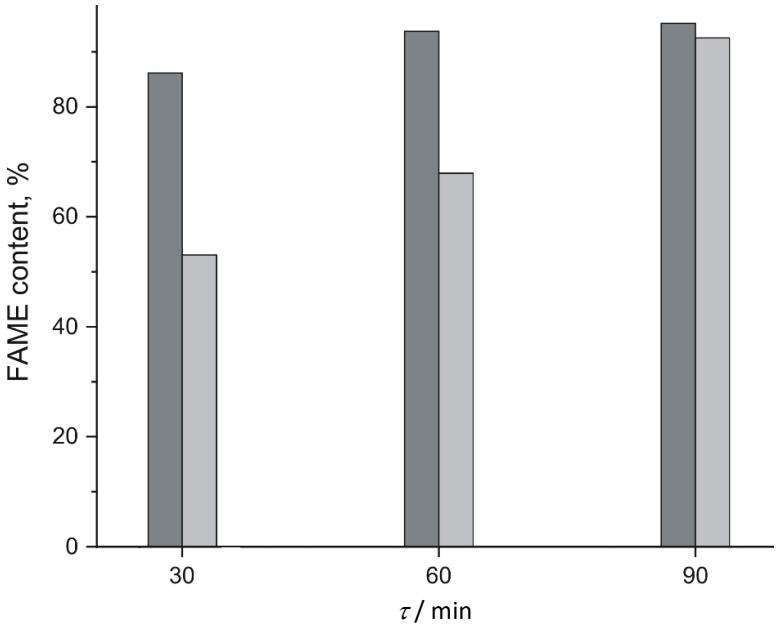

Fig. 7. Comparison of FAME contents obtained by using the fresh PSSA (dark grey) and recalcined PSSA (light grey) as catalysts at different reaction times (temperature of 60 °C, methanol-to-oil molar ratio of 12:1, and catalyst amount of 10 %)

5. CONCLUSION

Waste plum stones can be a significant raw material for biodiesel production as they can be used as a source of oil (kernels) and catalyst (stone shell ash). However, using plum oil in transesterification required its pre-esterification because of its high acid value and basic properties of the catalyst. The plum stone shell ash predominantly contains K, Ca, and Mg compounds. The catalytic test revealed that PSSA at 60 °C was the most active catalyst as compared to PSA and PKCA. The determined activation energy value (58.8 kJ mol^{-1}) was in the range of the values reported for ash-based catalysts. Overall, PSSA can be recommended as a catalyst for biodiesel production from plum kernel oil because of its efficiency and reusability after recalcination.

Acknowledgments: The present work has been funded by the Ministry of Science, Technological Development and Inovation of the Republic of Serbia, Program for financing scientific research work, No. 451-03-47/2023-01/200133.

REFERENCES

[1] Banković-Ilić IB, Stamenković OS, Veljković VB. Biodiesel production from non-edible plant oils. *Renew Sust Energ Rev* 2012; 16(6): 3621-3647. https://doi.org/10.1016/j.rser.2012.03.002

[2] Chen K, Wang J, Dai Y, Wang P, Liou C, Nien C, Wu J, Chen C. Rice husk ash as a catalyst precursor for biodiesel production. *J Taiwan Inst Chem Eng*. 2013; 44(4): 622-629. http://dx.doi.org/10.1016/j.jtice.2013.01.006

[3] Miladinović, MR, Krstić JB, Zdujić MV, Veselinović LjM, Veljović DjN, Banković-Ilić IB, Stamenković OS, Veljković VB. Transesterification of used cooking sunflower oil catalyzed by hazelnut shell ash. *Renew Energy*. 2022; (183): 103-113. https://doi.org/10.1016/j.renene.2021.10.071

[4] Petković M, Miladinović M, Banković-Ilić I, Stamenković O, Veljković V. Optimization of the used sunflower oil methanolysis catalyzed by hazelnut shell ash. *Adv Technol*. 2021; 10(2): 32-39. https://doi.org/10.5937/savteh2102032P

[5] Miladinović MR, Krstić JB, Ivana B. Banković-Ilić, Vlada B. Veljković, Stamenković OS. Valorization of walnut shell ash as a catalyst for biodiesel production. *Renew Energy*. 2020; 147: 1033-1043. https://doi.org/10.1016/j.renene.2019.09.056

[6] Fatimah I, Purwiandono G, Sahroni I, Sagadevan S, Chun-Oh W, Ghazali SAISM, Doong R. Recyclable catalyst of ZnO/SiO_2 prepared from *Salacca* leaves ash for sustainable biodiesel conversion. *South African J Chem Eng.* 2022; 40: 134–143. https://doi.org/10.1016/j.sajce.2022.02.008

[7] Fatimah I, Taushiyah A, Najah FB, Azmi U. ZrO_2/bamboo leaves ash (BLA) catalyst in biodiesel conversion of rice bran oil. *Mater Sci Eng.* 2018; 349: 012027. https://doi.org/10.1088/1757-899X/349/1/012027

[8] Fatimah I, Yanti I, Totok E. Suharto TE, Sagadevan S. ZrO_2-based catalysts for biodiesel production: A review. *Inorg Chem Commun.* 2022; 143: 109808. https://doi.org/10.1016/j.inoche.2022.109808

[9] Wang L, Yu H. Biodiesel from Siberian apricot (*Prunus sibirica* L.) seed kernel oil. *Biores Technol* 2012; 112: 355-358, https://doi.org/10.1016/j.biortech.2012.02.120

[10] Rashid U, Rehman H A., Hussain I, Yusup S. Production and characterization of biodiesel produced from musk melon (*Cucumis melo*) seed oil. In: BIT's 1st Annual World Congress of Bioenergy (WCBE 2011), 25-30 April 2011, Dalian, China.

[11] Chu J, Xu X, Zhang Y. Production and properties of biodiesel produced from *Amygdalus pedunculata* Pall. *Biores Technol*. 2013; 134: 374-376. https://doi.org/10.1016/j.biortech.2012.12.089

[12] Schinas P, Karavalakis G, Davaris C, Anastopoulos G, Karonis D, Zannikos F, Stournas S, Lois E. Pumpkin (*Cucurbita pepo* L.) seed oil as an alternative feedstock for the production of biodiesel in Greece. *Biomass Bioenerg*. 2009; 33(1): 44-49, https://doi.org/10.1016/j.biombioe.2008.04.008

[13] Rashid U, Ibrahim M, Yasin S, Yunus R, Taufiq-Yap Y-H, Knothe G. Biodiesel from *Citrus reticulata* (mandarin orange) seed oil, a potential non-food feedstock. *Ind Crops Prod.* 2013; 45: 355-359, https://doi.org/10.1016/j.indcrop.2012.12.039

[14] *Crops and livestock products*, Food and Agriculture Organization of the United Nations, https://www.fao.org/faostat/en/#data/QCL accessed November 3, 2022

[15] Saeed A, Hanif MA, Haq Nawaz RWKQ. The production of biodiesel from plum waste oil using nano-structured catalyst loaded into supports. *Sci Rep*. 2021; 11: 24120. https://doi.org/10.1038/s41598-021-03633-w

[16] Kostić MD, Veličković AV, Joković NM, Stamenkovic OS, Veljkovic VB. Optimization and kinetic modeling of esterification of the oil obtained from waste plum stones as a pretreatment step in biodiesel production. *Waste Manag*. 2016; 48: 619-629. https://doi.org/10.1016/j.wasman.2015.11.052

[17] Górna P, Rudzi M, Soliven A. Industrial by-products of plum *Prunus domestica* L . and *Prunus cerasifera* Ehrh. as potential biodiesel feedstock: Impact of variety. *Ind Crops Prod*. 2017; 100: 77-84. https://doi.org/10.1016/j.indcrop.2017.02.014

[18] Vicente G, Martinez M, Aracil J, Esteban A. Kinetics of sunflower oil methanolysis. *Ind Eng Chem Res.* 2005; 44: 5447-5454. https://doi.org/10.1021/ie040208j

[19] Vicente G, Martinez M, Aracil J. Kinetics of *Brassica carinata* oil methanolysis. *Energ Fuels* 2006; 20: 1722-1726. https://doi.org/10.1021/ef060047r

[20] Georgogianni KG, Kontominas MG, Pomonis PJ, Avlonitis D, Gergis V. Alkaline conventional and in situ transesterification of cottonseed oil for the production of biodiesel. *Energ Fuels.* 2008; 22: 2110-2115. https://doi.org/10.1021/ef700784j

[21] Jamil AZ, Muslim A. Performance of KOH as a catalyst for transesterification of *Jatropha curcas* oil. *Int J Eng Res Appl*. 2012; 2: 635-639. ISSN: 2248-9622

[22] Rabu RA, Janajreh I, Honnery D. Transesterification of waste cooking oil: Process optimization and conversion rate evaluation. *Energ Conv Manag*. 2013; 65: 764-769. https://doi.org/10.1016/j.enconman.2012.02.031

[23] Kostić MD, Joković NM, Stamenković OS, Veljković VB. Biodiesel production from seed oil of cotton thistle (*Onopordum acanthium* L.). *Adv Technol*. 2014; 3: 35-45. UDK 62.756.3:66.061.34:582.998.1 (In Serbian)

[24] Stamenković OS, Kostić MD, Joković NM, Veljković VB. The kinetics of base-catalyzed methanolysis of waste cooking oil. *Adv Technol*. 2015; 4(1): 33-41. https://doi.org/10.5937/savteh1501033S

[25] Kostić MD, Stamenković OS, Veljković VB. The influence of fatty acid composition on the kinetics of the vegetable oil methanolysis reaction. *Adv Technol*. 2021; 10(2): 24-31. https://doi.org/10.5937/savteh2102024K

[26] Mares EKL, Matheus A, Teresa P, Rafael L. Acai seed ash as a novel basic heterogeneous catalyst for biodiesel synthesis: Optimization of the biodiesel production process. *Fuel*. 2021; 299: 120887. https://doi.org/10.1016/j.fuel.2021.120887

[27] Sitepu EK, Sembiring Y, Supeno M, Tarigan K, Ginting J, Karo-karo JA, Tarigan JB. Homogenizer-intensified room temperature biodiesel production using heterogeneous palm bunch ash catalyst. *South African J Chem Eng*. 2022; 40: 240–245. https://doi.org/10.1016/j.sajce.2022.03.007

[28] Pathak G, Das D, Rajkumari K, Rokhum L. Exploiting waste: Towards a sustainable production of biodiesel using: *Musa acuminata* peel ash as a heterogeneous catalyst. *Green Chem*. 2018; 20(10): 2365-2373. https://doi.org/10.1039/C8GC00071A

[29] Husin H, Abubakar A, Ramadhani S, Sijabat CFB, Hasfita F. Coconut husk ash as heterogenous catalyst for biodiesel production from *Cerbera manghas* seed oil. MATEC Web of Conferences, The 3rd Annual Applied Science and Engineering Conference. Bundung, Indonesia, 2018, vol. 197, p. 09008. https://doi.org/10.1051/matecconf/201819709008

[30] de Barros S, Pessoa Junior WAG, Sá ISC, Takeno ML, Nobre FX, Pinheiro W, Manzato L, Iglauer S, de Freitas FA. Pineapple (*Ananás comosus*) leaves ash as a solid base catalyst for biodiesel synthesis. *Bioresour Technol*. 2020; 312: 123569. https://doi.org/10.1016/j.biortech.2020.123569

[31] Vargas EM, Ospina L, Neves MC, Tarelho LAC, Nunes MI. Optimization of FAME production from blends of waste cooking oil and refined palm oil using biomass fly ash as a catalyst. *Renew Energ*. 2021; 163: 1637-1647. https://doi.org/10.1016/j.biortech.2020.123569

[32] Adepojua TF, Ibeha MA, Babatunde EO, Asuquo AJ, Abegunde GS. Appraisal of CaO derived from waste fermented-unfermented kola nut pod for fatty acid methylester (FAME) synthesis from *Butyrospermum parkii* (Shea butter) oil. *South African J Chem Eng* 2020; 33: 160–171. https://doi.org/10.1016/j.sajce.2020.07.008

[33] Hsiao M-C, Liao P-H, Lan NV, Hou S-S. Enhancement of biodiesel production from high-acid-value waste cooking oil via a microwave reactor using. *Energies*. 2021; 14: 437. https://doi.org/10.3390/en14020437

[34] Miladinović MR, Stamenković OS, Veljković VB, Skala DU. Continuous sunflower oil methanolysis over quicklime in a packed-bed tubular reactor. *Fuel*. 2015; 154: 301-307. https://doi.org/10.1016/j.fuel.2015.03.057

[35] Veljković VB, Stamenković OS, Todorović ZB, Lazić ML, Skala DU. Kinetics of sunflower oil methanolysis catalyzed by calcium oxide. *Fuel*. 2009; 88: 1554–1562. https://doi:10.1016/j.fuel.2009.02.013

[36] Nath B, Kalita P, Das B, Basumatary S. Highly efficient renewable heterogeneous base catalyst derived from waste Sesamum indicum plant for synthesis of biodiesel. *Renew Energy*. 2020; 151: 295-310. https://doi.org/10.1016/j.renene.2019.11.029

[37] Vassilev S V., Vassileva CG, Song YC, Li WY, Feng J. Ash contents and ash-forming elements of biomass and their significance for solid biofuel combustion. *Fuel*. 2017; 208: 377-409. https://doi.org/10.1016/j.fuel.2017.07.036

[38] Vassilev S V, Baxter D, Vassileva CG. An overview of the behaviour of biomass during combustion : Part II. Ash fusion and ash formation mechanisms of biomass types. *Fuel*. 2014; 117: 152-183. https://doi.org/10.1016/j.fuel.2013.09.024

[39] Zdujić M, Lukić I, Kesić Ž, Janković-Častvan I, Marković S, Jovalekić Č, Skala D. Synthesis of $CaOSiO_2$ compounds and their testing as heterogeneous catalysts for transesterification of sunflower oil. *Adv Powder Technol*. 2019; 30: 1141-1150. https://doi.org/10.1016/j.apt.2019.03.009

[40] Emeruwa E, Jarrige J, Mexmain J, Bernardin M. Application of mercury porosimetry to powder (UO_2) analysis. *J Nucl Mater*. 1991; 184(1): 53-58. https://doi.org/10.1016/0022-3115(91)90532-C

[41] Lukić I, Krstić J, Jovanović D, Skala D. Alumina/silica supported K_2CO_3 as a catalyst for biodiesel synthesis from sunflower oil. *Bioresour Technol*. 2009; 100: 4690-4696. https://doi.org/10.1016/j.biortech.2009.04.057

[42] Yang P, Zhou S, Du Y, Li J, Lei J. Self-assembled meso / macroporous phosphotungstic acid/TiO_2 as an efficient catalyst for oxidative desulfurization of fuels. *J Porous Mater*. 2017; 24: 531-539. https://doi.org/10.1007/s10934-016-0288-7

[43] Fraile JM, García N, Mayoral JA, Pires E, Roldán L. The basicity of mixed oxides and the influence of alkaline metals: The case of transesterification reactions. *Appl Catal A: General*. 2010; 387: 67-74. https://doi.org/10.1016/j.apcata.2010.08.002

[44] Buchori L, Istadi I, Purwanto P, Marpaung LC, Safitri RL. Roles of K_2O on the CaO-ZnO catalyst and its influence on catalyst basicity for biodiesel production. *E3S Web Conf ICENIS 2017*. 2018; 31(3): 02009. https://doi.org/10.1051/e3sconf/20183102009

[45] Tang Y, Liu H, Ren H, Cheng Q, Cui Y, Zhang J. Development KCl/CaO as a catalyst for biodiesel production by tri-component coupling transesterification. *Sust Energ*. 38(2); 2018: 647-653. https://doi.org/10.1002/ep.12977

[46] Mendonça IM, Paes OARL, Maia PJS, Souza MP, Almeida RA, Silva CC, Duvoisin S, de Freitas FA. New heterogeneous catalyst for biodiesel production from waste tucumã peels (*Astrocaryum aculeatum* Meyer): Parameters optimization study. *Renew Energy*. 2019; 130: 103-110. https://doi.org/10.1016/j.renene.2018.06.059

[47] Betiku E, Mistura A, Victor T. Banana peels as a biobase catalyst for fatty acid methyl esters production using Napoleon's plume (*Bauhinia monandra*) seed oil: A process parameters optimization study. *Energy.* 2016; 103: 797-806. https://doi.org/10.1016/j.energy.2016.02.138

[48] Luque R, Pineda A, Colmenares JC, Campelo JM, Romero AA, Serrano-Riz JC, Cabeza LF, Cot-Gores J. Carbonaceous residues from biomass gasification as catalysts for biodiesel production. *J Nat Gas Chem*. 2012; 21(3): 246-250. https://doi.org/10.1016/S1003-9953(11)60360-5

[49] Chouhan APS, Sarma AK. Biodiesel production from *Jatropha curcas* L. oil using *Lemna perpusilla* Torrey ash as heterogeneous catalyst. *Biomass Bioenerg*. 2013; 55: 386-389. https://doi.org/10.1016/j.biombioe.2013.02.009

[50] Ho WWS, Kiat H, Gan S, Huey S. Evaluation of palm oil mill fly ash supported calcium oxide as a heterogeneous base catalyst in biodiesel synthesis from crude palm oil. *Energ Conv Manag*. 2014; 88: 1167-1178. http://dx.doi.org/10.1016/j.enconman.2014.03.061

[51] Roschat W, Siritanon T, Yoosuk B, Promarak V. Rice husk-derived sodium silicate as a highly efficient and low-cost basic heterogeneous catalyst for biodiesel production. *Ener Conv Manag*. 2016; 119: 453-462. https://doi.org/10.1016/j.enconman.2016.04.071

[52] Nath B, Das B, Kalita P, Basumatary S. Waste to value addition: Utilization of waste Brassica nigra plant derived novel green heterogeneous base catalyst for effective synthesis of biodiesel. *J Clean Prod*. 2019; 239: 118112. https://doi.org/10.1016/j.jclepro.2019.118112

[53] Changmai B, Rano R, Vanlalveni C, Rokhum L. A novel *Citrus sinensis* peel ash coated magnetic nanoparticles as an easily recoverable solid catalyst for biodiesel production. *Fuel*. 2021; 286: 119447. https://doi.org/10.1016/j.fuel.2020.119447

Korišćenje otpadnih koštica šljive kao izvora ulja i katalizatora za proizvodnju biodizela

Marija R. Miladinović[1], Stefan Pavlović[2], Ivana B. Banković-Ilić[1], Milan D. Kostić[1], Olivera S. Stamenković[1] i Vlada B. Veljković[1,3]

[1]Tehnološki fakultet, Univerzitet u Nišu, Bulevar Oslobodjenja 124, 16000 Leskovac, Srbija
[2]Univerzitet u Beogradu, Institut za hemiju, tehnologiju i metalurgiju, Centar za katalizu i hemijsko inženjerstvo, Njegoševa 12, 11000 Beograd, Srbija
[3]Srpska akademija nauka i umetnosti, Knez Mihailova 35, 11000 Beograd, Srbija

(Naučni rad)

Izvod

U ovom radu istraživana je mogućnost korišćenja otpadnih koštica šljive u proizvodnji biodizela. Jezgra šljive su iskorišćena kao sirovina za dobijanje ulja primenom Soxhlet-ove metode ekstrakcije. Cele koštice, ljuske koštica šljive i pogača dobijena nakon ekstrakcije ulja iz jezgra šljive spaljeni su da bi se dobio pepeo, koji je korišćen kao katalizator. Dobijene tri vrste sakupljenog pepela su najpre okarakterisane u pogledu hemijskog sastava, poroznosti i baznosti, a zatim je testirana katalitička aktivnost u transesterifikaciji esterifikovanog ulja koštica šljive. Dominantni elementi u pepelu, kao što su kalijum, kalcijum i magnezijum, imali su različit sadržaj u sve tri vrste pepela. Najveću katalitičku aktivnost pokazao je pepeo koštica šljive, zbog čega je dalje istraživan uticaj temperature (40, 50 i 60 °C) na brzinu reakcije katalizovane ovim pepelom. Konstanta brzine reakcije povećavala se sa porastom temperature reakcije, a vrednost energije aktivacije je 58,8 kJ mol^{-1}. Pored toga, pepeo koštica šljive može se ponovo koristiti kao katalizator nakon rekalcinacije.

Ključne reči: pepeo; kataliza; kinetika; metanoliza; transesterifikacija